

PV-STATCOM based Power Oscillation Damping and Simultaneous Fast Frequency Control by Utilizing PVSolar System

Sayyad Iram Ayaz Ali 1, Prof. S.S.Hadpe 2

1 Student of Electrical (Power system) Matoshree college of engineering

2 Professor of Electrical (Power system) Matoshree college of engineering

Abstract -The environmental protection aspect promoted the use of renewable energies at a faster rate over the last decade. Among all the renewable energy sources one of the most popular one is solar energy source. The application of these sources to the grid requires additional compensating devices for mitigate the power quality problems and ensure voltage stability. The flexible AC transmission system includes various compensating devices. This paper deals with the utilization of solar PV farm inverter as a static compensator (STATCOM) to regulate voltage at the point of connection which improves the stability both during day and night time. A linearized state space model of PV-STATCOM is developed to show the benefits of PV-STATCOM controls over Smart PV inverter controls in the presence of control system interaction between dc-link voltage and point of common coupling voltage controllers. These benefits are further substantiated by comparing the performance of PV-STATCOM and Smart PV inverter to perform voltage control during system disturbances simulated by irradiance changes and faults The proposed PV solar system working as a STATCOM is known as PV-STATCOM.

Key Words: Photovoltaic (PV) System, Smart PV inverter, PV-STATCOM, Voltage Flicker, Transient Voltage Changes, State Space Model, Dynamic Reactive Current Injection.

I. INTRODUCTION

Utilities are presently facing a major challenge of grid integrating an increasing number of renewable- energy-based distributed generators (DGs) while ensuring stability, voltage regulation, and power quality.[1] application of a grid connected PV solar farm inverter as a PV-STATCOM, during both night and day for increasing transient stability and

consequently, the power transmission limit of long transmission line. It utilizes the entire solar farm inverter capacity during the night and the remainder inverter capacity after real power generation during the day; both of which remain unused in conventional solar farm operation. Similar STATCOM control functionality can also be implemented in inverter based wind turbine generators during no-wind or partial wind scenarios for improving the transient stability of the system. Studies are performed for two variants of a Single Machine Infinite Bus (SMIB) system.[2]

Photovoltaic (PV) Energy is being widely adopted in globally because it is pollution free; maintenance free and abundant in nature. Its growth is rapid worldwide; which has been resulted in 25-35% annual growth rate in last ten years. Solar PV appears as a reliable; cost-competitive and sustainable electricity source in a growing number of countries. Due to innovative research in semiconductor technology PV prices decrease by 40% in the last several years. STATCOM is a Voltage Source Converter (VSC) based Flexible AC Transmission System (FACTS) device. It can provide dynamic reactive power compensation with a response time of 1-2 cycles, and can provide rated reactive current for voltages as low as 0.2 pu. The utilization of PV solar farm as STATCOM, termed PV- STATCOM, was demonstrated for increasing the connectivity of neighbouring wind farms and enhancing the power transmission capacity during night and day.[5] A novel inverter controller is proposed to operate the PV solar system as STATCOM utilizing the rated inverter capacity during nighttime and the inverter capacity remaining after real power generation during daytime. This allows full utilization of the expensive asset of the PV solar during the entire 24-hr period.[4] With the development of distributed generation systems, the renewable electricity from PV sources became a resource of energy in great demand. The current

control scheme is mainly used in PV inverter applications for real power and reactive power control schemes. The emergence of wind generation is the leading source of renewable energy in the power industry, Wind farms totalling hundreds, even thousands, of MW are now being considered.[1]

A conventional grid connected Photovoltaic PV solar farm utilizes an inverter for converting the DC power output from PV arrays into AC power to be supplied to the grid. The STATCOM (a FACTS device) is also based on a voltage sourced converter which functions both as an inverter and rectifier. A novel control technology was proposed by which a PV solar farm can be operated as a STATCOM in the night time as well as during day. During the night time the entire inverter capacity of the PV solar farm is utilized as STATCOM, whereas during the day, the inverter capacity remaining after real power generation is utilized for STATCOM operation.[2]

As a part of power quality improvement program; Installation of Distributed Generation (DG) in captive manner has increased at receiving end to support the energy demands of nonlinear loads. It is a new form of support for electrical power system. The benefit of DG is that it can reduce costs of transmission and distribution lines by reducing its losses. Power electronics based converters plays major role in the distribution generation and integration of renewable energy resources like solar; wind into the power system.[3] optimal utilization of PV solar system inverter as a STATCOM for voltage control and power factor correction during both nighttime and daytime. A novel inverter controller is proposed to operate the PV solar system as STATCOM utilizing the rated inverter capacity during nighttime and the inverter capacity remaining after real power generation during daytime. This allows full utilization of the expensive asset of the PV solar during the entire 24-hr period. This has the potential to provide additional financial benefits to the PV solar system owners.[4]

A unique concept of utilizing PV solar farms as STATCOM during nighttime for providing different grid support functions as well as for providing the same benefits during daytime with inverter capacity remaining after real

power generation was proposed in 2009. STATCOM is a Voltage Source Converter (VSC) based Flexible AC Transmission System (FACTS) device. It can provide dynamic reactive power compensation with a response time of 1-2 cycles, and can provide rated reactive current for voltages as low as 0.2 pu. The utilization of PV solar farm as STATCOM, termed PV- STATCOM, was demonstrated for increasing the connectivity of neighbouring wind farms and enhancing the power transmission capacity during night and day. The controller design of a Voltage Source Converter based Distribution STATCOM (D-STATCOM) on an RTDS and its subsequent laboratory implementation with DSP/FPGA platform.[5]

II. VOLTAGE FLICKER DUE TO FLUCTUATION

In real power generated by PV systems Voltage flicker is defined as the low frequency variations in voltage in distribution networks. They are caused by industrial loads such as arc furnaces, welding systems, electric boilers etc.[6] that draw fluctuating power at low frequencies. The concept of voltage flicker has now been extended to many kinds of voltage fluctuations through the use of short term flicker assessment and long term flicker assessment [7].

Voltage flicker is also caused in distribution system by rapid fluctuations of real power supplied by PV system due to cloud passing [7]. This is also one of major issues that occur in distribution networks due to high penetration of PV systems. This issue also serves as one of the barriers that limits the interconnection of PV based renewable energy power system [8]. The flicker limit for 100 % drop in irradiance is considered to be 3 % based on the assumption that this drop occurs once per hour. In Figure 1.1, 3% is the limit for borderline of visibility of flicker when the voltage dip occurs once per hour. The same limit has been adopted for the voltage flicker studies in this thesis.

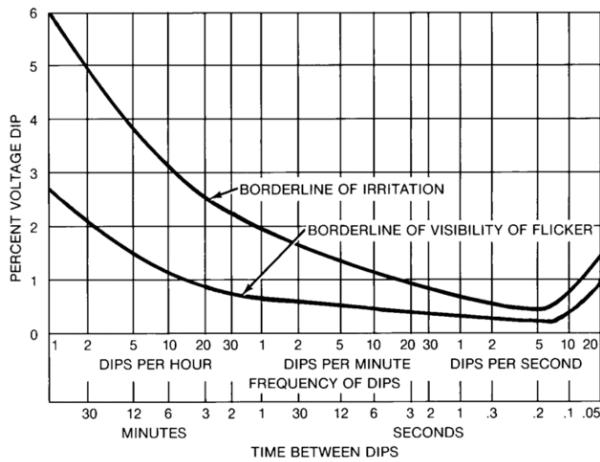


Figure1. Voltage flicker curve

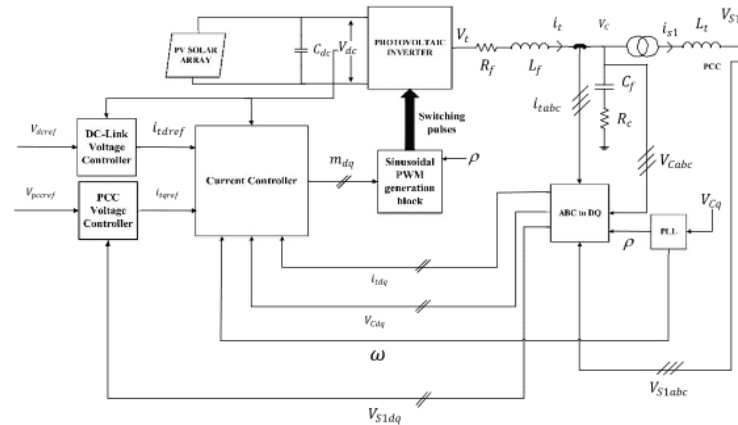


Figure2. Model of a Smart PV Inverter

III. MODELLING OF SMART PV INVERTER

Voltage Deviation (pu)

The model of a smart PV inverter incorporates the features of a conventional PV system and includes other components, depending on the smart functions to be implemented. The use of a smart PV inverter for voltage control is studied in this thesis and hence, the model with voltage control functionality is utilized for studies. A size and number of PV inverters used in a PV power plant will depend on its rating. For large power system studies, the entire PV power plant is represented by a single equivalent PV system [10].

The quantities and variables presented in Figure 3.1 are described as follows: C_{dc} is the DC link capacitance, V_{dc}

is the DC link voltage of PV system, V_t is the inverter terminal voltage, R_f is the sum of equivalent ON state resistance of power electronic component used in photovoltaic inverter and damping resistor of low pass filter, L_f is filter inductance, C_f is filter capacitance, R_c is also a damping resistor of low pass filter, i_t is the inverter output current, V_c is the voltage at the output of filter, i_{s1} is the output current of coupling transformer, V_{s1} is voltage at the output of coupling transformer (PCC voltage), L_t is the equivalent leakage inductance of coupling transformer, ρ is angle reference generated by phase locked loop (PLL) to synchronize PV system with the frequency of PCC which is represented by ω_p . ρ is also required for conversion of signals from abc to dq frame [11]. The signals with subscripts abc and dq represent the corresponding signals in the respective frames.

of electronic components are found in modern industrial equipment, like optical devices, programmable logic controllers, and adjustable speed drives. As the electronics components are very sensitive to voltage disturbances, the power utility company must guarantee the quality of power delivered to customers.

The voltage support provided by dynamic reactive current injection during LVRT requires the measurement of voltage at the point of grid connection and injection of reactive current by PV system at the low voltage side of interconnection transformer [12]. This basically involves measuring the PCC voltage and controlling the reactive current output of PV inverter [13].

IV. FFR AND POD CONTROLLER

A. Modified Plant controller (Repc)

The PV plant controller is set to POI voltage regulation model and plant real power control model.

1) Curtailment Logic

A Curtailment Logic is added in Fig. to the Repc to generate the plant real power reference, P_{plant_ref} . The Curtailment Logic enables curtailment of real power generation of the PV plant by a pre-specified amount $x\%$ (e.g. 50%) over a pre-specified time interval, t_1 . $P_{available}$ is the maximum available power from the PV plant. If there is no need for curtailment $x = 0$.

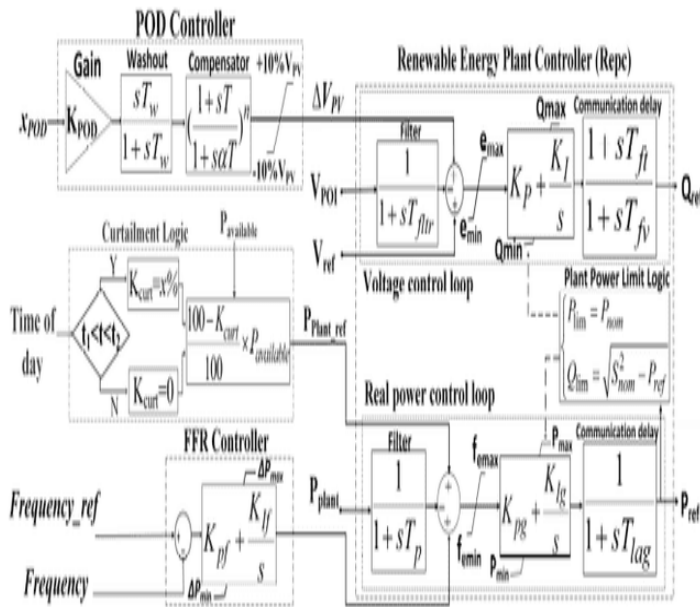


Figure.3 Simultaneous FFR and POD control scheme in a PV-STATCOM plant controller

2) Plant Power Limit Logic

To the best of authors’ knowledge, real/reactive power limits in the plant level control, Repc, are not dynamic in the current WECC generic dynamic models, i.e. the plant level reactive power limits are constant regardless of the available capacity. Since this paper proposes a novel plant-level real/reactive power modulation, a dynamic power limit logic is added to Repc. Priority is given to real power for which the limit is set to inverter nominal power, i.e. Plim. Thereactive power limit, Qlim, is dynamically calculated.

B. Power Oscillation Damping (POD) controller

The proposed POD controller consists of a washout filter, phase compensator and gain.

$$x_{out} = K_{POD} \frac{sT_w}{1+sT_w} \left(\frac{1+sT}{1+s\alpha T} \right)^n x_{POD}$$

C. Fast Frequency Response (FFR) controller

The proposed FFR controller acts on the real power of the PV-plant ΔPPV. The POI frequency is fed to the FFR controller and compared with reference value f0. A PI controller is used to eliminate the frequency error Δf, with the available PV plant real power capacity:

$$\Delta P_{PV} = \left(K_{pf} + \frac{K_{if}}{s} \right) (f - f_0)$$

V. SIMULATION RESULTS

The performance of the proposed composite FFR+POD controller is evaluated through time domain simulations in this section. Frequency deviations are classified as under frequency (generation less than demand) and over-frequency

(Generation more than demand) events. Over-frequency events can be readily mitigated by rapid reduction of the PV plant real power production. In contrast, under-frequency support is more challenging, since PV plants need to keep a percentage of available power as reserve capacity. As a result, the available support depends on the selected level of curtailment. Fig.5 shows the P and Q capability curves of the study PV system over the course of a day. The solid curves in Fig. show real and reactive power production curves when the curtailment logic in Fig. curtails the power in time span t1-t2. As a point in case, during the noon hours, the PV plant is generating 50MW instead of available 100MW power, i.e. Kcurt=50%, and this allows 100MVar reactive power capacity. Five different scenarios are simulated:

- 1) No control: neither FFR nor POD is performed. The PV plant operates only in dynamic voltage control mode.
- 2) POD control: only POD controller is active.
- 3) FFR control: only FFR controller is active.
- 4) FFR+POD control: Both FFR and POD controls are active. This study is the main contribution of this paper, which demonstrates the best realistic response possible from a PV solar plant.
- 5) Ideal control: Only POD controller is active. It is assumed that the time instant of occurrence and magnitude of the power imbalance are exactly known; and the PV solar farm compensates the imbalance instantaneously. This assumption is not made

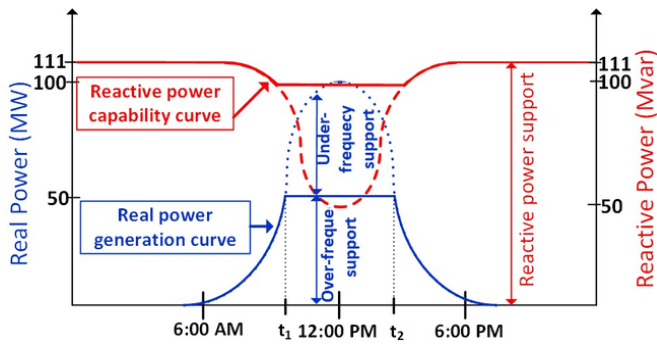


Figure4. Capability curves of the PV plant used as PV-STATCOM over the course of a day (dotted/dashed lines: peak power generation mode; Solidlines: curtailed mode)

A. Over-frequency control

1) 25 MW Load Trip in Area 1 (Pavailable=100 MW, Kcurt=0) Fig. 4 shows the behavior of the system when a 25 MW load is rejected in area 1 while PV plant generates 100 MW. Figs. 7(a)-(f) depict POI frequency (Hz), power transferred from area 1 to 2 (MW), PV plant real power (MW), PV plant reactive power (MVar), POI voltage (pu), PV plant current (pu), respectively. Fig. 4(a) shows that in No control case the frequency rises to around 60.06 Hz. When POD controller is activated, the oscillations in frequency are stabilized in less than 4s, but the frequency deviation is the same as in No control case. With FFR controller, the frequency deviation is less than 36 mHz. Nevertheless, inter-area oscillations still exist in the system frequency. The proposed FFR+POD controller stabilizes both frequency excursion and inter-area oscillations, making the response very close to that of the Ideal controller. Fig. 4(b) shows that with no POD controller, inter-area power oscillations in tie-line power continue for more than 20s.

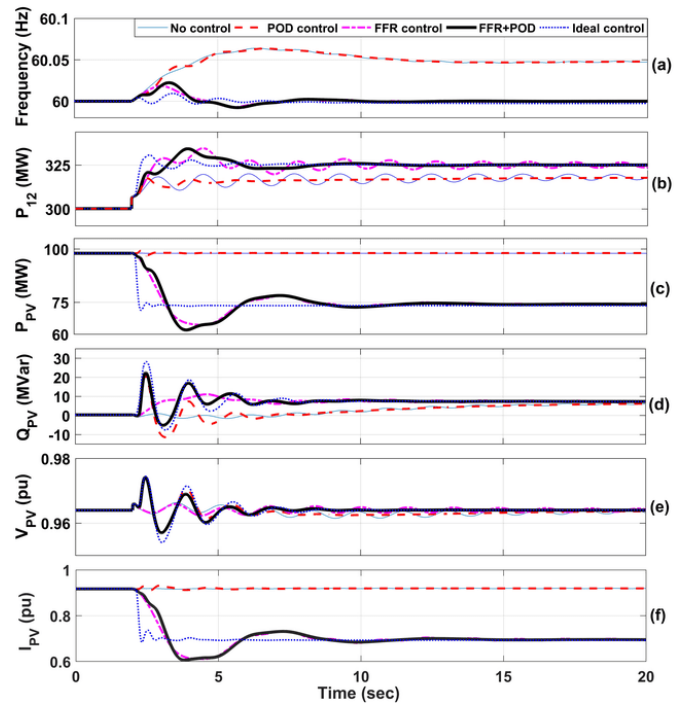


Figure 5. MW load rejection in area 1 (Pavailable=100 MW, K=0): (a) POI (Bus 8) frequency (b) Transferred power from area 1 to area 2 (c) PV plant real power (d) PV plant reactive power (e) PV-plant voltage (f) PV-plant current

2) 200 MW Load Trip in Area 1 (Pavailable=100 MW, Kcurt=0)

Fig. 5 shows the results of 200 MW load disconnection. The variables depicted are correspondingly similar to Fig. 5. except PV plant current that is not shown here. Since the PV plant is operating at its nominal power (100 MW), it can mitigate only 100 MW of the generation surplus, whereas the synchronous generators compensate the remaining power surplus (100 MW). Fig. 5.(a) illustrates that with the proposed FFR+POD control, peak of frequency is reduced from 60.37 Hz to 60.2 Hz. Furthermore, the frequency settles at 60.1 Hz compared to 60.27 Hz in No control and POD control cases. As demonstrated in Fig.5.(b), the FFR+POD controller also stabilizes inter-area oscillations in about 7s. Fig. 5.(c) shows that for such a large power imbalance, the FFR controller acts very rapidly (comparable with Ideal control) to reduce the PV real power to zero in less than a second.

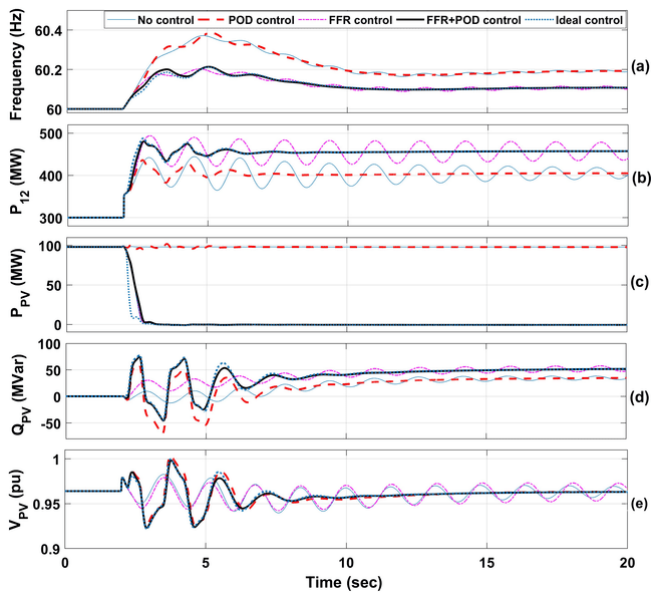


Figure.6. 200 MW load rejection in area 1 (Pavailable=100 MW, K=0): (a) POI(Bus 8) frequency (b) Transferred power from area 1 to area 2 (c) PV plant real power (d) PV plant reactive power (e) PV plant voltage

3) 200MW Load Trip in Area 1 (Pavailable=60 MW, Kcurt=0) Fig.6 shows the simulation results when PV plant is generating 60 MW and a 200 MW load is tripped in area 1. The variables depicted are correspondingly similar to Fig. 6 but PV plant current is not shown. Fig. 6 (a) demonstrates that in No control and POD control cases, system frequency rises to around 60.38 Hz and settles at 60.2 Hz similar to Fig. 6(a). However, in FFR, FFR+POD, and Ideal control cases, frequency rise is 60.26 Hz compared to 60.2 Hz of the previous study and settles at 60.1 Hz because of less over frequency support in this case (60MW vs 100MW). Fig. 6(b) shows the tie-line power.

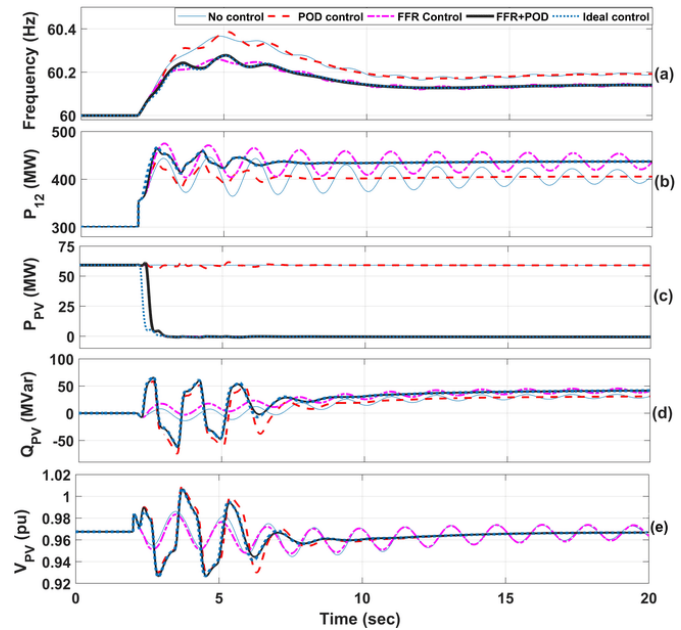


Figure7. 200 MW load rejection in area 1 (Pavailable=60 MW, K=0): (a) POI(Bus 8) frequency (b) Transferred power from area 1 to area 2 (c) PV plant real power (d) PV plant reactive power (e) PV plant voltage

B. Under frequency control

To provide frequency support during under-frequency events, the power output of the PV plants is curtailed as shown in Fig. 7 (solid curve). The PV solar system can then utilize this reserve capacity to compensate the generation deficiency during under-frequency scenarios. Curtailment of real power releases additional inverter capacity for reactive power exchange, which is used for providing effective voltage control and/or POD. For the studies in this section, the PV plant is curtailed by 50%, i.e. $K_{curt} = 50\%$, and simulations are conducted for available PV power of 100 MW. Another under-frequency simulation study 3) is also performed for an operating point when it is not noon, i.e. when the power output is less than the rated output (100 MW), i.e. $K_{curt} = 50\%$, Pavailable 60MW. This is done to investigate the sensitivity to operating conditions which may be more realistic than noon time.

1) 25 MW Load Connection in Area 1 (available=100 MW, $K_{curt} = 50\%$)

Fig. 7 demonstrates the results of a 25 MW sudden load increase in area 1, which initiates an under-frequency event. The variables depicted are correspondingly similar to

Fig. 7. As shown in Fig. 7 (a), the frequency drops to 59.94 Hz without FFR control. However, this frequency deviation is restricted to only 20 mHz with the proposed FFR control. Fig. 7 (b) depicts that inter-area oscillations decay when POD controller is applied. The transferred power from area 1 to 2 is reduced by about 12.5 MW in No control and POD cases because of the equal share of both the areas in compensating generation insufficiency. However, with FFR control, the power export from area 1 is reduced by 25 MW to supply the increased load in area 1. Fig. 7 (c) also shows that the PV plant rapidly increases its real power output to 75 MW. The remaining inverter capacity makes available 82 MVar reactive power modulation capability for POD. Fig. 7 (d) shows that the PV plant absorbs reactive power in steady-state to avoid the voltage rise (due to power transfer reduction). Fig. 7 (e) shows that the POI voltage oscillations settle down within 5% steady state value in 8 sec. Fig. 7 (f) demonstrates the PV plant current. The PV plant current is initially around 0.47 pu as the PV plant is curtailed by 50%.

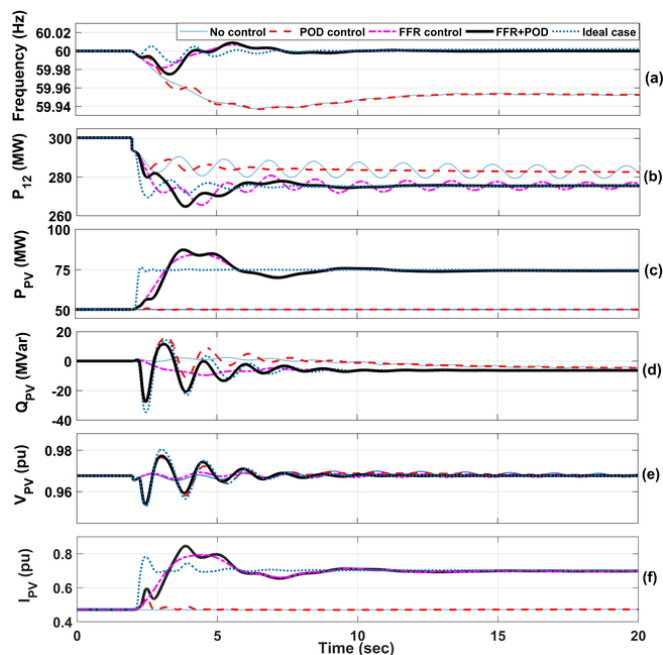


Figure 8. 100 MW load increase in area 1 (Pavailable=100 MW, K=50%): (a) PO(Bus 8) frequency (b) Transferred power from area 1 to area 2 (c) PV plant real power (d) PV plant reactive power (e) PV plant voltage (f) PV plant current

2) 100 MW Load Connection in Area 1 (Pavailable=100 MW, Kcurt=50%)

Fig. 8 presents the simulation results for a 100 MW sudden increase in load of area 1. The variables illustrated are correspondingly similar to Fig. 5.1, except PV plant current that is not shown. Fig. 8(a) shows that the FFR controller quickly releases 50 MW reserved power thereby alleviating the frequency nadir from 59.83 Hz to 59.91 Hz. Fig. 8(b) demonstrates that power oscillations decay in less than 8s with POD controller. Fig. 8(c) depicts that the PV plant effectively increases its power output from 50 MW to 100 MW in less than 1s. Fig. 8(d) shows that even though the available reactive power capacity is minimum in this case as 100 MVA of inverter capacity is used up for real power output, the power oscillations are stabilized in less than 8s. Fig. 8(e) illustrates effective voltage regulation simultaneously with POD. These results show that even with minimum available reactive power from PV plant, the proposed FFR+POD controller successfully provides improved frequency regulation, POD and voltage control in less than 8s.

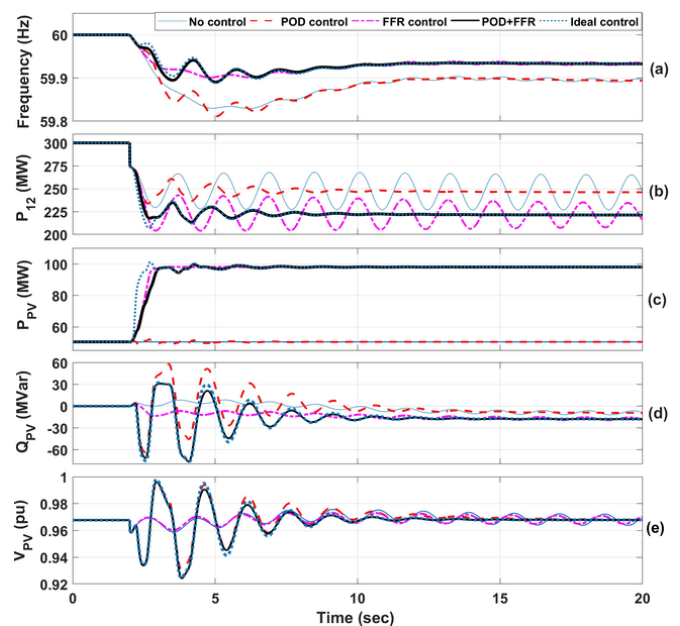


Figure 9. 100 MW load increase in area 1 (Pavailable=100 MW, K=50%): (a) POI (Bus 8) frequency (b) Transferred power from area 1 to area 2 (c) PV plant real power (d) PV plant reactive power (e) PV plant voltage

3) 100 MW Load Connection in Area 1 (Pavailable =60 MW, Kcurt=50%)

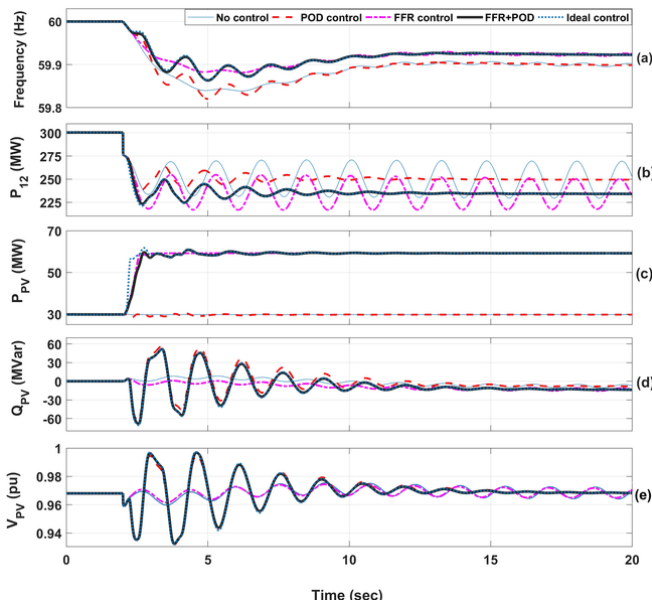


Figure 10. 100 MW load increase in area 1 ($P_{available}=60$ MW, $K=50\%$): (a) POI (Bus 8) frequency (b) Transferred power from area 1 to area 2 (c) PV plant real power (d) PV plant reactive power (e) PV plant voltage

Fig. 10 presents the simulation results of 100 MW connection in area 1, when available PV power is 60 MW. The PV plant is curtailed by 30 MW, i.e. $K_{curt} = 50\%$. As shown in Fig. 10(a), the frequency drops to 59.84 Hz without FFR control. However, in FFR, FFR+POD, and Ideal control cases, the frequency nadir reaches 59.89 Hz and settles at 59.93 at steady state. Compared to results of Fig. 10(a), with lower frequency support both the frequency nadir and steady-state frequency fall further. Fig. 10(b) depicts the transferred power. The POD controller effectively stabilizes the power oscillations in less than 6s. Fig. 10(c) demonstrates that PV plant is initially operating at 30 MW. When FFR controller is applied the 30 MW reserve power is used to support the system frequency. Figs. 10(d) shows the reactive power modulations for power oscillation damping. It is seen that in case of FFR+POD, the magnitude of reactive power modulation is higher compared to Fig. 10(d). This is mainly because of larger PV reactive power capacity.

C. Performance Comparison of Proposed Combined FFR+POD Control with Conventional Frequency Control

This study demonstrates the efficacy of the proposed FFR+POD controller as compared to the conventional (5%) droop control which is recommended by NERC for all generators including PV plants [40]. The comparison is made

for an under-frequency event during high level of tie-line power flow of 550 MW. The power output of PV plant is tailed by 50%. A load increase of 100 MW is initiated in area 2. The results are demonstrated in Fig. 10(a) which has similar description of variables as in Fig. 10(b) show that the conventional droop-based controller has very little impact on the system frequency, whereas the FFR controller noticeably reduces the frequency deviation. The ineffectiveness of droop control can be understood by observing the PV plant real power variation in Fig. 10(c). Only a minor real power contribution (~5 MW) is made by the PV plant operating with 5% droop, which mainly corresponds to its size with respect to the conventional generators (100 MW vs. 2800 MW of synchronous generation). In No control case, load increase in area 2 leads to a rise in tie-line power which destabilizes the system as shown in Fig. 10(b). The droop control has no positive impact on dynamic stability. The FFR controller preserves system stability although the tie line power is highly oscillatory. The proposed FFR+POD controller enhances system damping, so that the power oscillations decay in less than 5s. It is seen from Fig. 10(d), that when FFR+POD control is activated, the system stability is maintained with lower reactive power injection. The system voltage variations shown in Fig. 10(e), are controlled in a significantly better manner with the proposed combined controller.

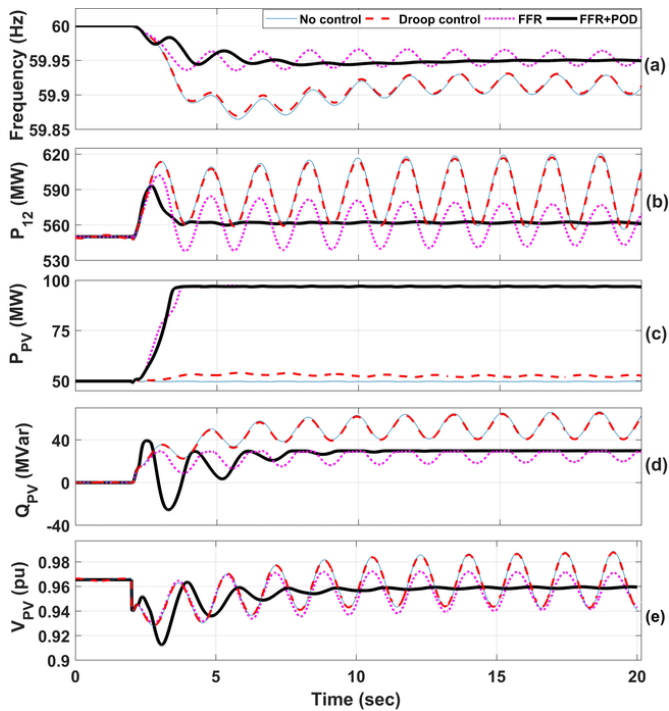


Figure 11. 100 MW load increase in area 2, PV plant output curtailed by 50%:

- (a) POI (Bus 8) frequency
- (b) Transferred power from area 1 to area 2
- (c) PV plant real power
- (d) PV plant reactive power
- (e) PV plant voltage

VI. CONCLUSIONS

Application of partial PV-STATCOM for performing voltage control to mitigate flicker in PCC voltage introduced by 100% change in irradiance. The PV system is made to perform PCC voltage control with feed-forward voltage filter time constants at 0.75 ms so that the interaction between dc-link voltage control loop and PCC-voltage control loop is at a maximum. The stability of proportional and PI controller based dynamic reactive current injections, and Volt/Var controls are compared.

There are many challenges involved in the grid integration of PV systems which are created by high penetration of PV systems. Smart PV inverters have been shown capable of mitigating some of the issues and increase the penetration level of PV systems in distribution networks. The smart inverter functions such as Volt/Var control, dynamic reactive current injection and low voltage ride through are some of the functions for voltage control purposes. It has been shown in this thesis these functions can also be implemented using PV-STATCOM controls.

Studies are also performed with two similar PV systems providing simultaneous voltage support during and post fault. The proportional controller based dynamic reactive current injection results in oscillatory PCC voltage responses post fault and this goes towards instability as the slope of dynamic reactive current injection characteristic increases. The PI controller results in a relatively better damped and stable response for all values of considered slopes.

VII. ACKNOWLEDGEMENT

Author would like to express gratitude and appreciation to her guide Er. Prof. S.S.Hadpe for his constant inspiration and valuable guidance. Author would like to thank to all those who gave her support and helped in understanding the subject.

REFERENCES

1. M. Arun Bhaskar, B. Vidya, S.S. Dash, C. Subramani, M. Jagadeesh Kumar Department of EEE, Velammal Engineering College Chennai, Tamil Nadu, "Application of Integrated Wind Energy Conversion System (WECS) and Photovoltaic (PV) Solar Farm as Statcom to Regulate Grid Voltage during Night Time".
2. K. Sujatha, M. Satyanarayana Pursuing M.Tech, PSCA Branch, Dept of EEE, Jayamukhi Institute of Technological Sciences, Narsampet, Warangal 2 Asst. Prof., EEE, Dept., Jayamukhi Institute of Technological Sciences, Narsampet, Warangal, "Control Application of PV Solar Farm as PV-STATCOM for Reactive Power Compensation during Day and Night in a Transmission Network", October 2016, Volume 3, Issue 10 JETIR (ISSN-2349-5162).
3. Niraj Solanki and Jatinkumar Patel Dept. Of Electrical Engg.; G.H. Patel College Of Engg. & Technology; Vallabh Vidyanagar, "Utilization Of PV Solar Farm For Grid Voltage Regulation During Night; Analysis & Control", IEEE International Conference on Power Electronics, Intelligent Control and Energy Systems (ICPEICES-2016).
4. Rajiv K. Varma, Senior Member IEEE, Byomakesh Das, Student Member IEEE, Iurie Axente and Tim Vanderheide, Member IEEE, "Optimal 24-hr Utilization of a PV Solar System as STATCOM (PV-STATCOM) in a Distribution Network".
5. Rajiv K. Varma, Senior Member, IEEE, and Ehsan M. Siavashi, Member, IEEE, "PV-STATCOM: A New Smart Inverter for voltage Control in Distribution System".
6. J. Gutierrez, J. Ruiz, A. Lazkano, and L. A. Leturiondo, "Measurement of Voltage Flicker: Application to Grid-connected Wind Turbines," in Advances in Measurement Systems, ed: InTech 2010.
7. C. Schauder, "Advanced Inverter Technology for High Penetration Levels of PV Generation in Distribution Systems," NREL Subcontract Report: NREL/SR5D00-60737, 2014.
8. F. Katiraei and J. R. Aguero, "Solar PV Integration Challenges," IEEE Power and Energy Magazine, vol. 9, pp. 62-71, 2011.
9. IEEE Recommended Practice for Electric Power Distribution for Industrial Plants, IEEE Std 141-1993, pp. 1-768, 1994.
10. Muljadi, M. Singh, and V. Gevorgian, "User Guide for PV Dynamic Model Simulation Written on PSCAD Platform," NREL Technical Report: NREL/TP5D00-62053, 2014.

11. A. Yazdani and R. Iravani, Voltage-Sourced Converters in Power Systems : Modeling, Control, and Applications. Hoboken, NJ: Wiley, 2010.
12. "Grid Code High and Extra High Voltage," E.ON Netz GmbH, April 2006.
13. A. Camacho, M. Castilla, J. Miret, J. C. Vasquez, and E. Alarcon-Gallo, "Flexible Voltage Support Control for Three-Phase Distributed Generation Inverters Under Grid Fault," IEEE Transactions on Industrial Electronics, vol. 60, pp. 1429-1441, 2013.